ORIGINAL PAPER

Stress Analysis for Rock Mass Failure with Offset Joints

Omer Mughieda · Maher T. Omar

Abstract Two-dimensional finite element model was created in this work to investigate the stress distribution within rock-like samples with offset open non-persistent joints under uniaxial loading. The results of this study have explained the fracture mechanisms observed in tests on rock-like material with open non-persistent offset joints (Mughieda and Alzo'ubi, Geotech Geol Eng J 22:545–562, 2004). Finite element code SAP2000 was used to study the stresses distribution within the specimens. Four-noded isoperimetric plain strain element with two degrees of freedom per node, and the three-noded constant strain triangular element with two degree of freedom per node were used in the present study. The results of the present study showed that the tensile stress in the bridge area caused coalescence for specimens with overlapped preexisting cracks (joints) while the coalescence of the secondary cracks, due to shear stress, caused the failure of specimens with non-overlapping cracks.

O. Mughieda (✉)
Department of Civil and Environmental Engineering, University of Sharjah, Sharjah, United Arab Emirates
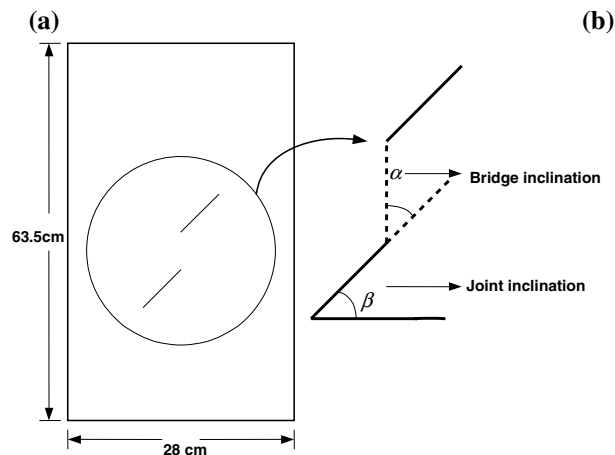e-mail: mughieda@just.edu.jo

M. T. Omar
Department of Civil Engineering, Intelligent Systems and Infrastructure & Energy and Environment Research Groups, University of Sharjah, P.O. Box 27272, Sharjah, United Arab Emirates
e-mail: momar@sharjah.ac.ae

1 Introduction

Fracture coalescence means the connection or merging of two or more fractures (joints or cracks) due to fracture propagation. Rock mass containing non-persistent joints can only fail if the joints propagate and coalesce through intact rock bridge. Shear strength of rock mass containing non-persistent joints is highly affected by both mechanical behavior and geometrical configuration of the non-persistent joints located in rock mass. The existence of rock joints and rock bridges is the most important cause for the complicated mechanical response of rock mass to stress loading. The joint-bridge interaction and bridge failure dominates the mechanical behavior of jointed rock masses and the stability of rock excavations. A number of experimental studies of fracture coalescence has been carried out such as Hoek and Bieniawski (1984) and Brace and Byerlee (1967) on glass, Lajtai (1974) on plaster of Paris, Horii and Nemat-Nasser (1986), Pollard and Aydin (1988), Reyes and Einstein (1990), Germanovich et al. (1995), Shen et al. (1995) and Bobet and Einstein (1998) on gypsum. Two types of crack patterns have been observed by those researchers: Wing cracks and secondary cracks. Wing cracks appear first; they are

tensile cracks, which initiate at the tips of the joint (from now on the term joint will be used for preexisting cracks) and propagate steadily in a curvilinear path in the direction of the applied axial load. Secondary cracks appear later and are responsible for specimen failure in most cases. Mughieda and Alzo'ubi (2004) performed uniaxial compression tests on block specimens made of rock like material (Portland cement: type I, water and sand) to study the effect of bridge inclination angle on the fracture mechanism of rock masses. The present finite element work has been carried out to investigate the stress distribution in the bridge area which was the most important reason for the coalescence of fracture and eventually the failure of the specimens.

2 Experimental Work

Mughieda and Alzo'ubi (2004) have performed a series of uniaxial compression tests on blocks with offset non-persistent joints to study the effect of bridge inclination angle on the failure mechanism of blocks with open non persistent rock joints. The inclination angle of the joints (β) remained constant at 45° for all specimens and the inclination angle of the bridge (α) was changed from 0.0 to 120° with an increment of 15°. The geometry of block tested and loading frame are shown in Fig. 1. The test results showed that for bridge inclination angle of 0° coalescence occurred due to shearing mode of failure. For bridge inclination angle of 30, 45, 90 and 105°, coalescence occurred due to mixed tensile and shear failure. For bridge inclination angle of 60, 75, and

Fig. 2 Upper side of failure surface of specimen with $\beta = 45°$ and $\alpha = 45°$ cracks. (Mughieda and Alzo'ubi 2004)

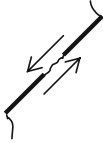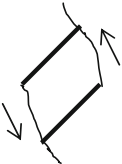120° coalescence was due to pure tensile failure. Figure 2 shows an example of block specimen with $\beta = 45°$ and $\alpha = 45°$ cracks after failure. Table 1 shows the geometry and mechanism of failure for the tested specimens.

3 Stress Analysis of Interacting Cracks

3.1 Description of Finite Element Models

In order to determine the state of stress before the wing crack initiation and coalescence, finite element analyses using FE code SAP2000 (Wilson and Habibullah 1989) were performed on the crack arrangements that were studied experimentally. A linear elastic material was assumed for these analyses, mainly because there were no signs of major material damage prior to crack initiation and

Fig. 1 (a) Geometry of the specimens and pre-existing cracks, (b) Loading frame. (Mughieda and Alzo'ubi 2004)

Table 1 Mode of Coalescence Observed in Different Specimens, (Mughieda and Alzo'ubi 2004)

α/β	Schematic path of coalescence	Description	Mode of coalescence
0/45		Crack coalescence occurred by shear cracking	Shear
30/45		Wing crack initiated from the inner tips of pre-existing crack and crack coalescence occurred by secondary crack propagation	Tension + Shear
45/45, 60/45		Crack coalescence occurred by shear crack which initiated in the middle of rock bridge during the wing crack propagated	Tension + Shear
90/45		Wing crack initiated from the inner tips of pre-existing crack and coalescence occurred by wing crack in the middle of pre-existing crack	Tension
105/45, 120/45		Wing crack initiated from the inner tips of pre-existing crack and coalescence occurred by wing crack in the outer tips of pre-existing crack	Tension + shear

coalescence. Modulus of elasticity of approximately 10510 MPa was obtained from the experimental load-displacement curves and used in the analyses. A Poisson's ratio of 0.25 was assumed.

Four-nodded isoperimetric plain strain element with two degree of freedom per node, and the three-nodded constant strain triangular element with two degree of freedom per node were used in the present study. Figure 3 shows an example of a finite element model for determining the stress field around pre-existing cracks (in this case, $\beta = 45°$ and $\alpha = 30°$).

The following boundary conditions were applied on the finite element model: zero vertical displacement along the bottom edge, and a uniform distribution load on the top surface, the magnitude of which was approximately the measured coalescence load (in MPa) for the crack geometry analyzed. It was assumed that the cracks were sufficiently far from the top and bottom of the block such that the exact distribution of loads on theses edges did not significantly affect the stresses around the cracks. The three-dimensional effects in the experiments were
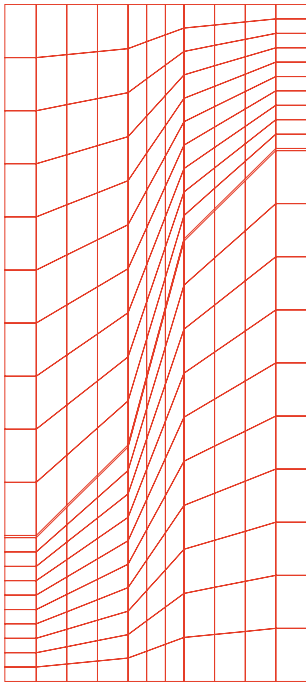
Fig. 3 Finite element model for determining stress field around 45°–30° cracks

Fig. 4 Maximum shear stresses around 45°–0° crack
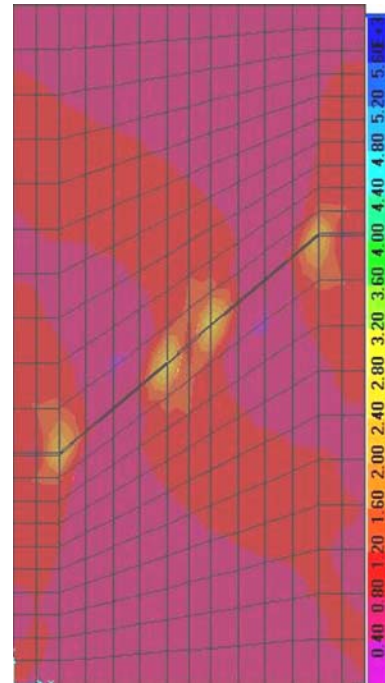
neglected since the model used in the present study was two-dimensional.

3.2 Linear Elastic Analysis Results and Discussion

3.2.1 Coplanar Joints (β = 45, α = 0°)

The finite element analysis showed that shear stress was maximum in the region between the pre-existing cracks (bridge segment). Which implies that the shear stress was mainly responsible for the initiation and propagation of the secondary crack that caused the specimen failure. Experimental work showed that there was a significant amount of pulverized and crushed materials and traces of shear displacement, indicated that a shearing failure had taken place. Figure 4 shows the shear stress distribution.

3.2.2 Slightly Offset Joints (β = 45, α = 30°)

Experiential work showed that shear and tensile stresses were both responsible for the crack initiation and propagation that caused failure of the sample.

Same conclusion can be reached by examining the results of finite element analysis. Figure 5 shows that the maximum tensile stress and maximum shear stress are both located in the bridge segment between the pre-existing cracks.

3.2.3 Offset Joints (β = 45, α = 45°)

Both experimental and finite element analyses coincided and showed that the shear stresses at the internal tip of the cracks and the tensile stresses in the bridge segment caused the initiation and propagation of the cracks that caused the failure of the specimen. Figure 6 shows maximum principal and maximum shear stresses in the specimen.

3.2.4 Sample with (β = 45, α = 60)

Experimental work showed that wing cracks were initiated at the inner tips of the pre-existing cracks and then followed by the initiation of the secondary cracks in the bridge segment between the pre-existing racks. Finite element analyses showed that high tensile stress existed at the inner tips of the cracks and
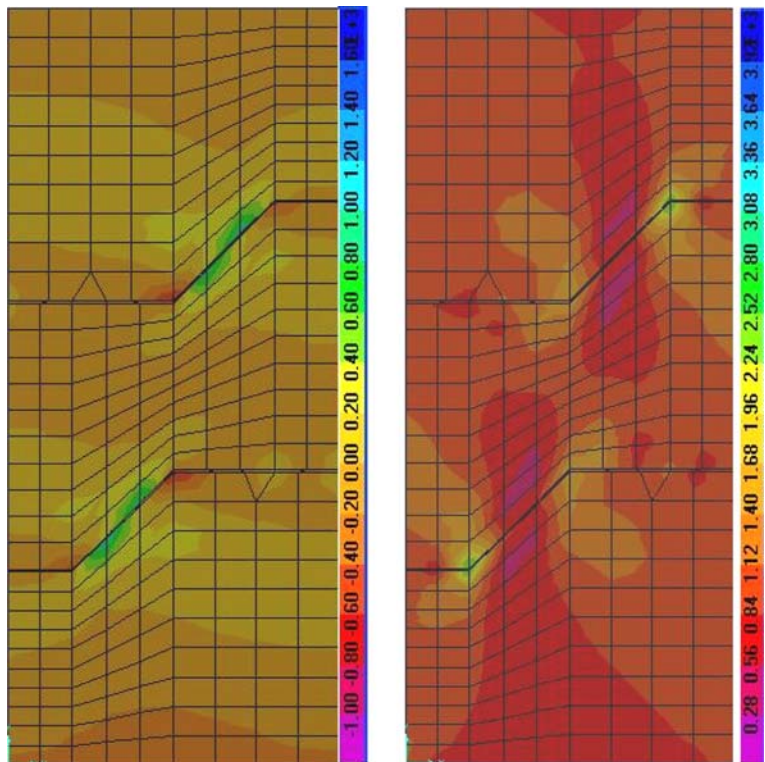
Fig. 5 (**a**) Maximum principal stress and (**b**) maximum shear stress around 45°–30° cracks
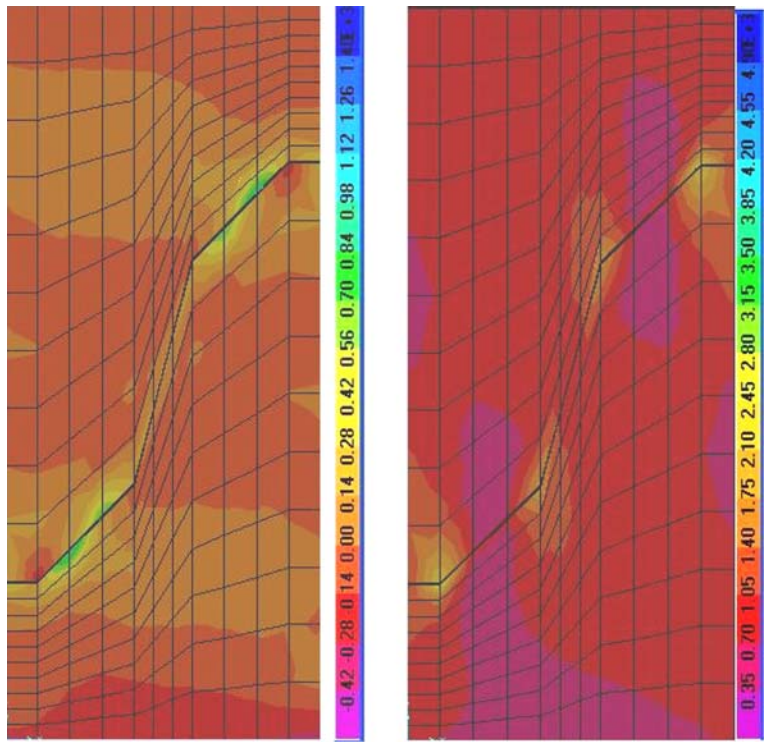
(a) Maximum principal stresses

(b) Maximum shear stresses

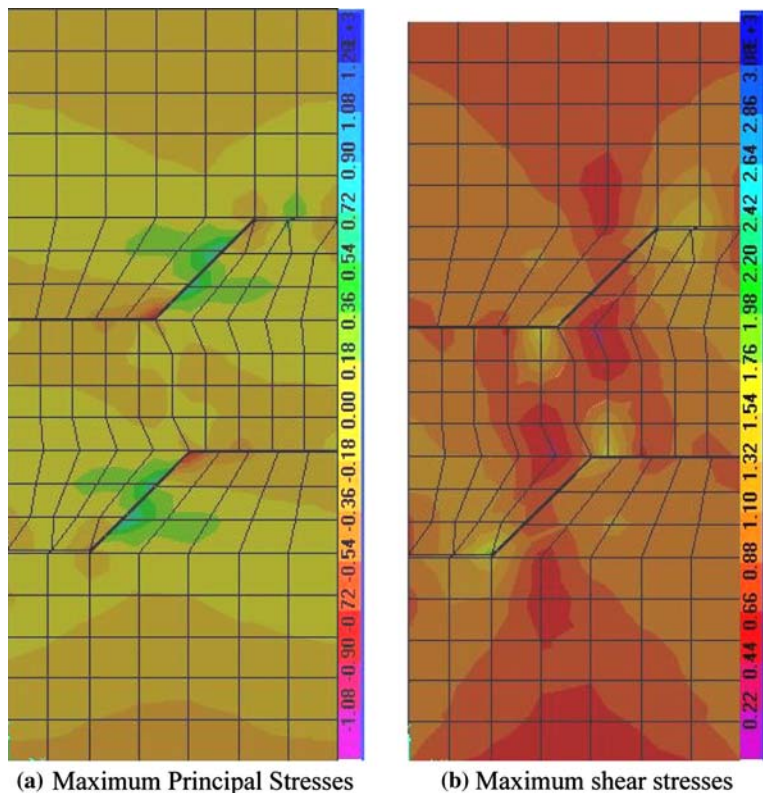**Fig. 6** (**a**) Maximum principal stress and (**b**) maximum shear stress around 45°–45° cracks

(a) Maximum Principal Stresses

(b) Maximum shear stresses

(a) Maximum Principal Stresses   (b) Maximum shear stresses

high shear stress existed in the bridge segment. Figure 7 shows the finite element analyses results.

3.2.5 Sample with ($\beta = 45$, $\alpha = 75°$)

Experimental work showed that failure of the specimen was due to coalescence of wing cracks that initiated at the inner tips of the pre-existing cracks and propagated stably in curvilinear path.

The surface of failure at the bridge area is tensile surface because no crushed or pulverized materials and no evidence of shear movement were noticed. The wing cracks surface also had the same characteristic of tension surface. Figure 8 shows the result of finite element analyses.

3.2.6 Sample with ($\beta = 45$, $\alpha = 90°$)

Failure of this specimen was due to coalescence of wing cracks as shown by experimental work which completely coincided with the results of finite element analyses which showed that tensile stress existed in the bridge segment between the pre-existing cracks as shown in Fig. 9.

3.2.7 Sample with ($\beta = 45$, $\alpha = 105°$)

In these samples the wing cracks were initiated and propagated stably. At the time of failure, a crack was initiated at the wing crack that started at the inner tip of the upper joint and propagated causing the sample failure. Small traces of shear displacement could be noticed at the first part of the crack that caused the failure. At the rest of that crack, tension characteristic could be detected. The surfaces of wing cracks were created in tension. Complicated shear-tensile stresses at the left side of the sample caused the failure. Figure 10 shows the results of finite element analyses while Fig. 11 shows the crack propagation and coalescence.

3.2.8 Sample with ($\beta = 45$, $\alpha = 120°$)

Wing cracks were initiated and propagated downward and upward. Wing cracks initiated another crack that started at the right side. All wing cracks at the right of the sample coalesced with each other forming continuous line of fracture while the crack

(a) Maximum Principal Stresses   (b) Maximum shear stresses

Fig. 8 (a) Maximum principal stress and (b) maximum shear stress around 45°–75° cracks

(a) Maximum principal stresses   (b) Maximum shear stresses
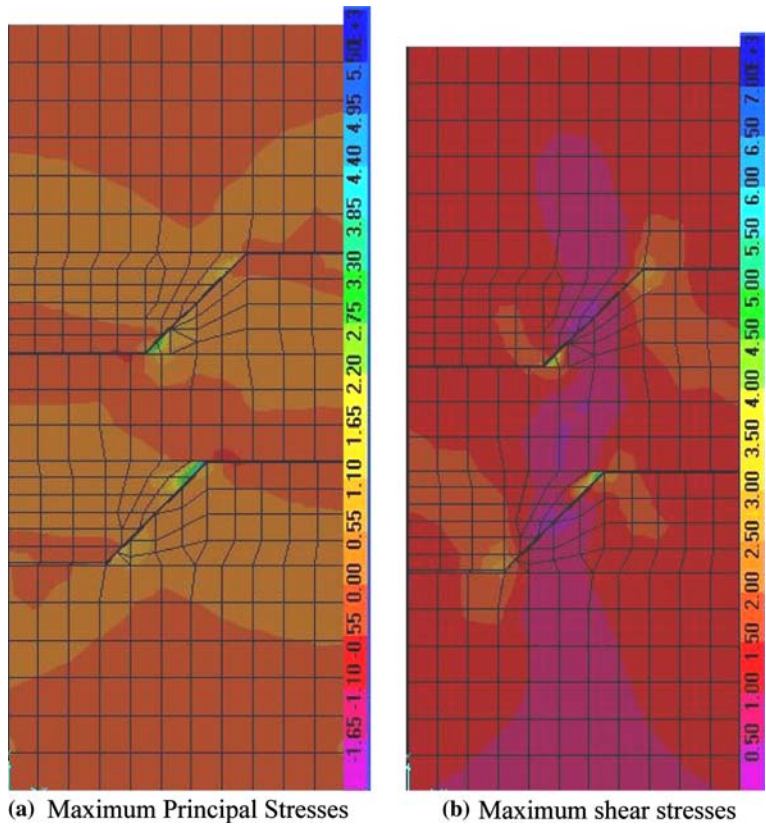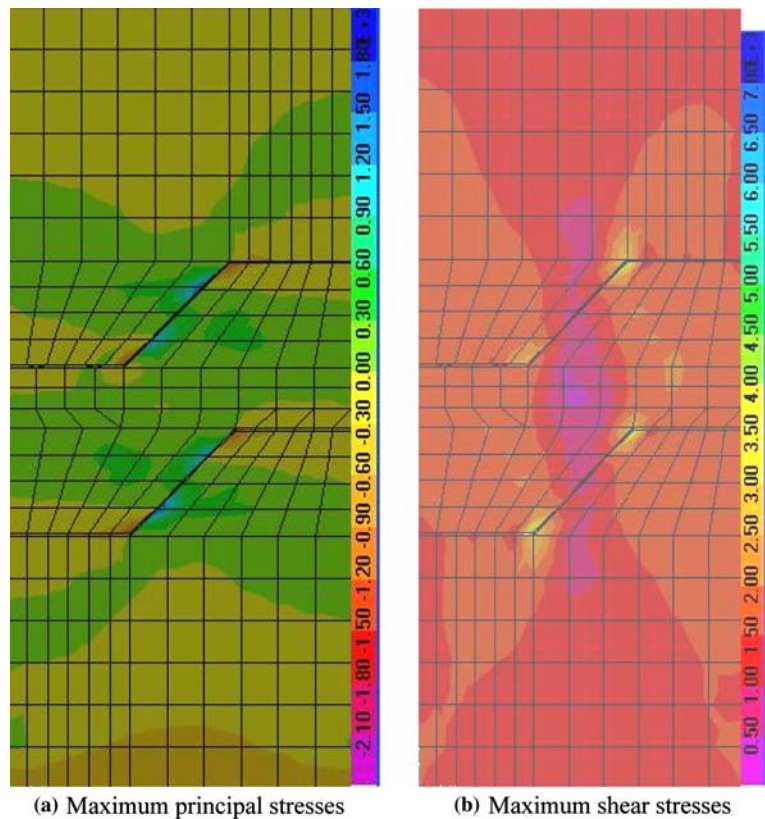
Fig. 9 (a) Maximum principal stress and (b) maximum shear stress around 45°–90° cracks
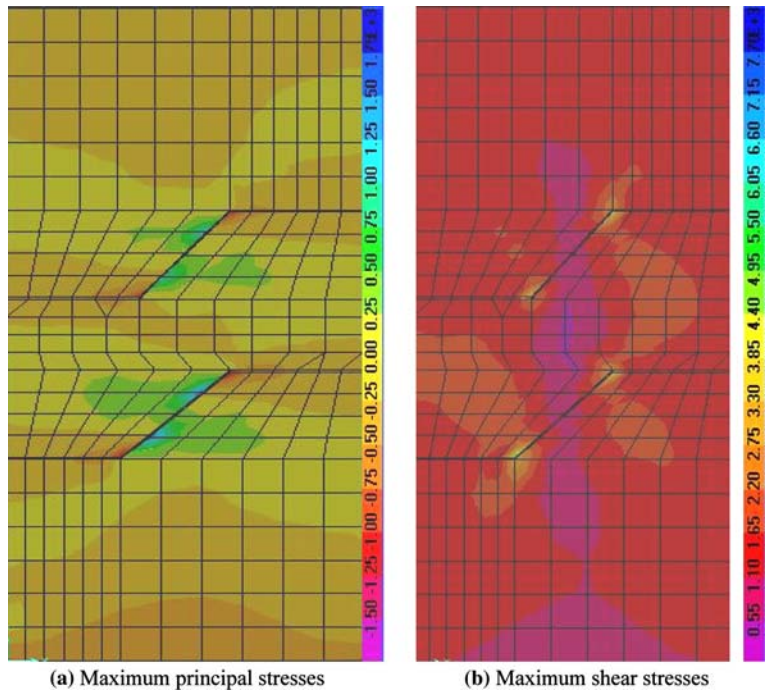
Fig. 10 (**a**) Maximum principal stress and (**b**) maximum shear stress around 45°–105° cracks

(a) Maximum principal stresses   (b) Maximum shear stresses
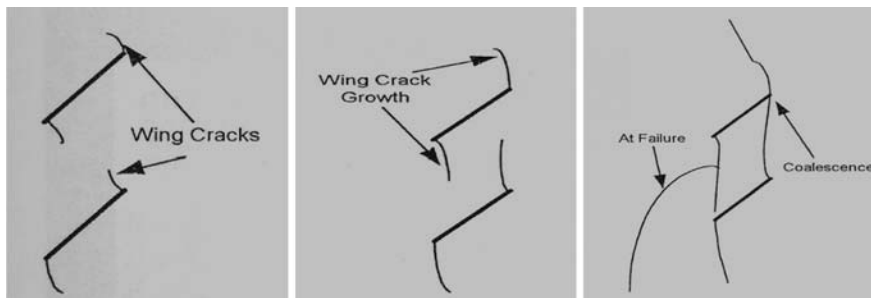
Fig. 11 Crack propagation and coalescence for ($\beta = 45$, $\alpha = 105°$). (Mughieda and Alzo'ubi 2004)

at the right side coalesced with the inner tip of upper joint and caused the sample to fail. Tensile stresses caused the sample failure.

The first part of the wing crack that initiated at the right side was created in shear while the rest of the crack was created by tensile stresses. Figure 12 shows the finite element analyses result while Fig. 13 shows the crack propagation and coalescence.

4 Conclusions

The failure of rock mass containing non-persistent joints is complicated and not well understood yet. Finite element analysis was performed to study the stresses condition at the tips of the pre-existing joints and in the rock bridge segments on crack arrangements that were studied experimentally. Two modes of failure were found in the experimental

Fig. 12 (**a**) Maximum principal stress and (**b**) maximum shear stress around 45°–120° cracks

(a) Maximum principal Stresses   (b) Maximum shear stresses
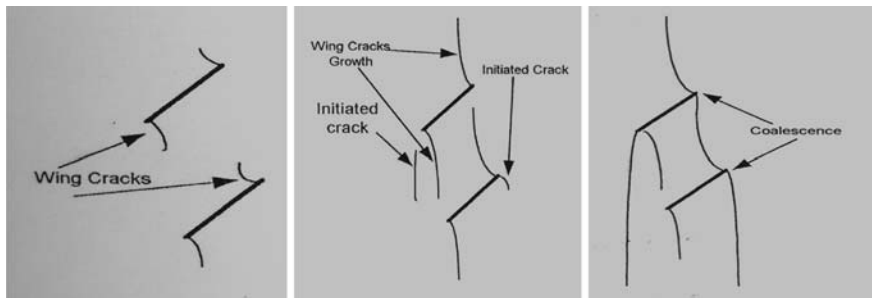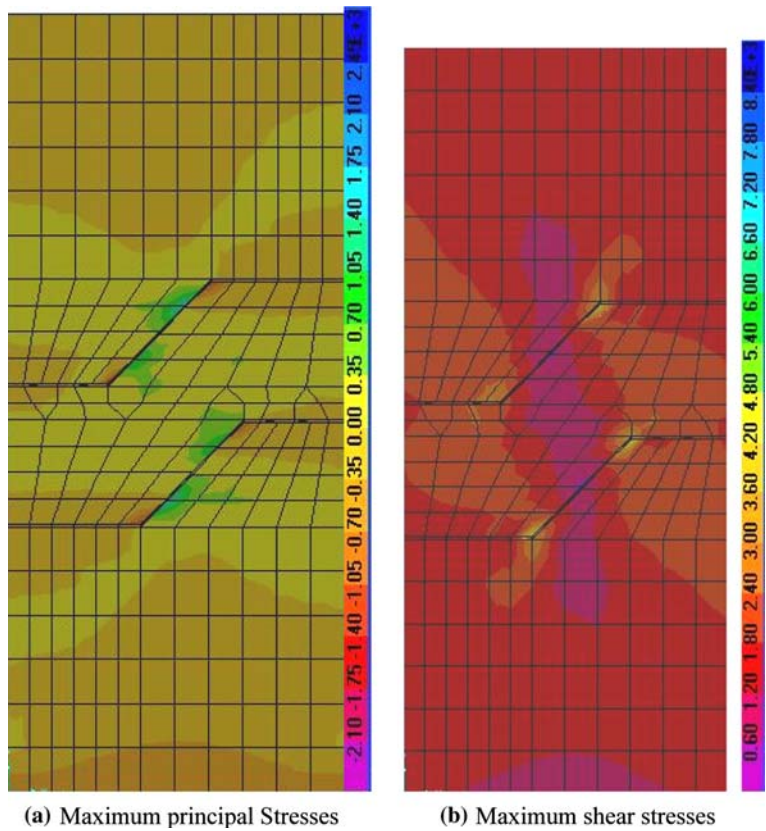
Fig. 13 Crack propagation and coalescence ($\beta = 45$, $\alpha = 120°$). (Mughieda and Alzo'ubi 2004)

study. The first was due to tensile stress and called wing crack while the other is the secondary crack and due to shear stress. Finite element analyses based on two-dimensional finite element model and linear elastic material showed that tensile stress was mainly responsible for wing crack initiation while the shear stress was responsible for the secondary crack initiation.

References

Bobet A, Einstein HH (1998) Fracture coalescence in rock-type materials under uniaxial and biaxial compression. Int J Rock Mech Min Sci 35:863–888

Brace W, Byerlee J (1967) Recent experimental studies of brittle fracture rocks. In: Fairhurst C (ed) Proceedings of the eighth symposium on rock mechanics, University of Minnesota, failure and breakage of rock, pp 57–81

Germanovich LN, Ring LM, Carter BJ, Ingraffea AR, Dyskin AV, Ustinov KB (1995) Simulation of crack growth and interaction in compression. Proceedings of the 8th International Congress on rock mechanics, vol 1. ISRM, Tokyo

Hoek E, Bieniawski ZT (1984) Brittle fracture propagation in rock under compression. Int J Fract 26:276–294

Horii H, Nemat-Nasser S (1986) Brittle failure in compression: splitting, faulting and brittle–ductile transition. Philos Trans R Soc Lond 319(1549):337–374

Lajtai E (1974) Brittle fracture in compression. Int J Fract 10:525–536

Mughieda O, Alzo'ubi A (2004) Fracture mechanisms of offset rock joints—a laboratory investigations. Geotech Geol Eng J 22:545–562

Pollard DD, Aydin A (1988) Progress in understanding jointing over the past century. Bull Geol Soc Am 100:1181–1204

Reyes O, Einstein HH (1990) Stochastic and centrifuge modeling of jointed rock, part I-fracturing of jointed rock. Final report submitted to the air force office of scientific research and air force engineering services center, 1990

Shen B, Stephanson O, Einstein HH, Ghahreman B (1995) Coalescence of fractures under shear stresses in experiments. J Geophys Res 100(B4):5975–5990

Wilson EL, Habibullah A (1989) SAP90 users manual. Computers and Structures Inc